Technology Development of a Novel Ka-band Digitally-Beamformed Interferometric Radar With Application to Ice Topography Mapping

Delwyn Moller, Yonggyu Gim, Brandon Heavey, Richard Hodges, Sembiam Rengarajan, Eric Rignot, Francois Rogez, Gregory Sadowy, Marc Simard, Mark Zawadzki

Jet Propulsion Laboratory, California Institute of Technology,
4800 Oak Grove Drive,
Pasadena, California 91109

***Abstract*— This paper discusses the innovative concept and technology development of a Ka-band (35 GHz) radar for mapping the surface topography of glaciers and ice sheets. Dubbed the "Glacier and Land Ice Surface Topography Interferometer" (GLISTIN) the system is a single-pass, single platform interferometric synthetic aperture radar (InSAR) with an 8mm wavelength, which minimizes snow penetration yet remains relatively impervious to atmospheric attenuation. Such a system has the potential for delivering topographic maps at high spatial resolution, high vertical accuracy, independent of cloud cover, with a subseasonal update and would greatly enhance current observational and modeling capabilities of ice mass-balance and glacial retreat.**

To enable such measurements, a digitally beamformed antenna array is utilized to provide a wide measurement swath at a technologically feasible transmit power. To prove this concept and advance the technology readiness of this design we are currently funded by the NASA ESTO Instrument Incubator Program to build and test a 1m x 1m digitally-beamformed Ka-band waveguide slot antenna with integrated digital receivers. This antenna provides 16 simultaneous receive beams, effectively broadening the swath without reducing receive antenna gain. The design and fabrication of such a large aperture at Ka-band presents many challenges, particularly achieving the phase stability required for digital beamforming and interferometric measurements. In this paper we will overview the system concept, requirements, status of the technology development and the experimental scenario by which the beamforming and interferometric performance will be demonstrated.

I. Introduction

This paper describes continuing the technology development effort of a novel Ka-band (35 GHz) radar that utilizes digital beamforming (DBF) over an elevation array in order to achieve significant savings in transmit power when compared with system requirements for a non-beamformed or scanned array that has the same swath illumination [1, 2].

The proposed application for this technology is focused toward interferometric mapping of glaciers and land-ice sheets with high precision and subseasonal complete coverage independent of cloud cover. The choice of Ka-band for these measurements is key, both in terms of the phenomenology and also the technology.

The "Glacier and Land Ice Surface Topography Interferometer" (GLISTIN) as we have called the system is depicted in Figure 1. The single-pass, single platform interferometric synthetic aperture radar (InSAR) has an 8mm wavelength, which minimizes snow penetration while incurring minimal attenuation due to the atmosphere. In contrast to lidars, the instrument will be insensitive to clouds, provide significant swath-widths, cover the poles sub-monthly, and provide inherently variable spatial resolution: high spatial resolution for sub-meter-scale vertical precision on glaciers and coastal regions; coarse spatial resolution for decimeter accuracy on featureless ice sheet interiors. Consequently this concept holds the potential for critical synoptic data not available from any equivalent system for observations, modeling and forecasting mass changes of the Earth's ice cover, as outlined in the Climate Variability and Change roadmap.

To date, no civilian spaceborne InSAR system has utilized Ka-band. Also, to our knowledge no digital beam forming radar has flown in space. This technology has no alternatives when high resolution and swath is required other than the use of extremely high power transmitters that are impractical from both a technological and power consumption standpoint (we achieve greater than an order of magnitude savings in power through the use of DBF). GLISTIN also results in a substantial mass savings when compared with a lower frequency system. For example, for equivalent accuracy at 13GHz (WSOA frequency) requires a boom of nearly 24m as opposed to the 8m of our design.

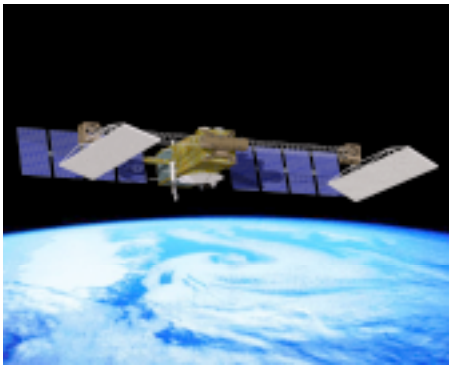

Figure 1: **GLISTIN mission concept.**

The GLISTIN IIP program is assessing mission design questions and within this context developing and demonstrating solutions to the key technological hurdles of the proposed satellite-based sensor. The most notable challenges are the large (4x1m) Ka-band digital beam-forming antenna array, systematic calibration and data processing. Initially we focused on the development of a mission scenario, and consequently science, system and instrument requirements. Currently in Year 2 of the 3-year program, we are continuing to look into spaceborne calibration issues, but are well into the technology development phase to meet the key requirements. Specifically we are designing, building, integrating and demonstrating a 1x1.1m (1/4 of the total spaceborne size) Ka-band digitally beamformed array with integrated digital receivers. This paper will describe the technology approach and current status of the development.

Section II reviews the science requirements and orbit selection that meets those requirements, followed by a summary of the spaceborne system design, and some prelimimary calibration results in Section III. Section IV then discusses the technology development status and shows some test results for both the slotted waveguide array prototype, and the digital receiver. We finish with a summary.

II. Science Requirements

The Greenland and Antarctic ice sheets together hold enough ice to raise global sea level by 80 m. The annual exchange of mass on the ice sheets is equivalent to 8mm/yr sea level, so that any fluctuation in that level of exchange is significant on a global scale.

Recent airborne laser altimetry campaigns, satellite radar altimetry, and ICESat altimetry in Greenland and Antarctica have revealed glacier thinning rates ranging from a few cm/yr in the interior to meters or tens of meters per year at the coast, along channels occupied by outlet glaciers. Most interior changes are explained in terms of fluctuations in snowfall, whereas large coastal changes are caused by glacier ice dynamics. While coastal changes dominate in Greenland and West Antarctica, changes in interior accumulation have a significant impact on total mass balance in East Antarctica; it is therefore important to monitor both interior and coastal regions. In order to obtain meaningful results on ice sheets based on existing observations and interpretation of the results, we estimate that surface elevation needs to be measured with a sub-10 cm accuracy on a 1 km scale in the interior, and a few tens of cm at a spatial resolution of 100m at the coast, where the km-scale dimensions of glaciers demand finer resolution. If these measurement objectives are achieved - namely better than 1m at 100 m resolution on glacier ice along the coast, less than 10 cm at 1 km resolution in the interior - one will be able to improve current estimates of ice sheet mass balance obtained from other altimetry techniques significantly. While measuring height changes over time is certainly a most important measurement to be made, there is also considerable value in assembling precise and complete topography of land-ice covered areas (requiring a mapping sensor rather than a profiler). This information provides constraints on the driving stress of the ice, drainage basins, and roughness statistics, as well as surface features that can be tracked through time to detect ice motion and acceleration. Given these motivations, Table 1 summarizes the science measurement and coverage requirements.

Table 1: Science and coverage requirements

Topic	Requirement
Coverage	Monthly to bi-monthly coverage of glaciers and ice-sheets
	Complete coverage of Antarctica and Greenland (a hole at the North Pole is acceptable)
Glaciers	100mx100m posting
	1m relative height accuracy
Ice-sheets	1km x 1km posting
	10 cm relative height accuracy

A. Orbit Selection

Based on the fundamental system concept combined with the science coverage requirements, an orbit of approximately 600km was selected with a resulting nominal ground swath of 70km (incidence angles ranging from 18.6-25.2 degrees). Initially sun-synchronous orbits were investigated and rejected as it was discovered that there was an unavoidable and unacceptable gap in coverage over both Poles. The coverage requirements in Table 1 call for full coverage of the South Pole – however a "hole" at the North Pole is acceptable: in a non-sunsynchronous near polar orbit, with a side-looking instrument a coverage gap is inevitable at one of the poles. Temperate glaciers are found close to the equator and it takes at least 571 swaths of 70 km each to cover the equator without gaps. This takes 39 days at 600km altitude for a 92 degree inclination and left-looking instrument, satisfying the monthly-bimonthly coverage requirement. The orbit was optimized to provide an evenly spread coverage after 1/2 repeat cycle and therefore guarantee two acquisitions every 1/2 repeat cycle above 60 degrees latitude. Based on this the best altitude/orbit count was a 605.7 km altitude, with 593 orbits/repeat cycle and a 40 day repeat period. It is notable that high latitudes (>60 degrees) are imaged every 10 days or better on average.

A consequence of employing a non-sun-synchronous orbit is that the spacecraft will transition into and out of eclipses. Eclipses impact both power resources and the thermal stability of the instrument itself. For any given initial sun geometry there will be 'eclipse seasons' when the satellite will go through the Earth's shadow for up to 35 min/orbit. During these seasons the average incident solar power will be reduced by up to 35% and batteries will be required to operate the radar during these eclipses. Calibration strategies to cope with the impact of eclipses on data coverage due to "thermal shock" will be examined as part of this program.

III. Spaceborne Instrument Design and Calibration Strategy

A. System Design Parameters

We have used the science requirements to design a radar system capable of simultaneously meeting all of the measurement requirements. The system parameters are summarized in Table 2. We have chosen a 0.063 m x 4.0 m transmit antenna to illuminate 7 degrees in elevation. At a boresight incidence angle of 22 degrees this results in a ground swath of 70 km. On receive, the full swath is synthesized as 16 simultaneous subswaths in elevation using DBF over the full receive antenna (1 x 4 m comprised of an array of sixteen 0.063 m x 4 m antenna "sticks" in elevation).

Table 2: Fundamental system parameters for the spaceborne interferometer

Parameter	Units	Quantity
Peak transmit Power	kW	1.5
Frequency	GHz	35
Bandwidth	MHz	80
Antenna Length	m	4
"stick" height	m	0.063
Number of sticks	#	16
Total Array Height	m	1.01
Pulsewidth	us	25
PRF	kHz	4
Interferometric baseline	m	8
Polarization		Horizontal
Swathwidth	km	70
Incidence angle range	degrees	18.6-25.2

The polarization of the antenna is chosen to be horizontal based on calculations of the antenna slot mutual coupling. The peak transmit power is 1.5kW, which is within the realm of currently available technology. The pulse repetition frequency is 4 kHz to satisfy critical sampling requirements. The bandwidth is kept relatively low (40MHz) to minimize data-rates yet satisfy glacial resolution goals. Despite this, the data-rate still presents a substantial challenge that we will address as a later part of this program.

B. Key Requirements Derivation

Within this program, requirement derivation serves the purpose of determining the specifications for the technology demonstration and development. The instrument requirements flow directly from the science requirements via instrument performance and resolution. In turn the instrument error budget is used to sub-allocate performance to subsystems. These errors comprise:

1. random errors due to thermal noise, ambiguities and multiplicative noise ratios
2. systematic errors
3. pointing errors

Table 3 summarizes the error budget rollup across the swath for the most stringent scenario; a 1km x 1km posting for wet snow and with a 5dB margin in signal to noise ration (SNR). Note that media (atmospheric and surface penetration) errors are currently ignored. One can see that the budget is very tight to meet the 10cm height accuracy requirement across the swath. It is likely the height precision will be improved due to the pessimistic nature of the assumptions. However the systematic/calibration errors are still significant contributors and levy stringent requirements upon the overall calibration and are very similar in magnitude to that derived for the Wide Swath Ocean Altimeter (WSOA) mission [3]. For this reason, it was concluded that a data calibration strategy using a nadir-viewing altimeter, similar to that developed for WSOA, would also be required for GLISTIN to meet the exacting requirements of the systematic error budget.

Table 3: Systematic error budget summary as a function of cross-track distance (CTD)

Error Source \ Cross Track Distance (km)	185	210	230	245
Height Precision (cm)	6.0	5.1	5.4	7.6
Systematic/Calibration Error (cm)	4.7	5.5	6.1	6.6
RSS Total Error (cm)	7.7	7.5	8.1	10.0

C. Calibration strategy

There are both geophysical and systematic contributions that can cause a bias (non-random) source of error (modeled in the allocation of Table 3 as an equivalent calibration accuracy). Primarily these can be summarized as:

1. Microwave penetration into the snow
2. Atmospheric (wet and dry troposphere) delay
3. Spacecraft attitude knowledge error
4. Baseline dilation knowledge error
5. Differential phase changes due to antenna thermal deformations

We have modeled the Ka-band microwave penetration into the snow as a function of the volumetric water content and for dry snow we have estimated this to be as high as 30cm. Therefore we need to estimate this penetration and correct for this bias. To do so backscatter will be used to estimate the wetness and therefore the penetration. However while the loss factor is well known for wet snow, this is not the case for dry snow, so field measurements from an airborne and/or ground-based campaign would be critical to refining this calibration model. We currently have proposals under consideration to make exactly such measurements.

Wet and dry tropospheric delays have yet to be characterized in terms of spatiotemporal variability. However, as an indication of order of magnitude and variability, initial calculations from coastal Antarctic radiosonde data collected throughout 2000 indicates centimetric level variability with wet delays of ~2cm+/-1cm and dry delays of ~226 cm +/-2cm. Note that in the interior regions of the ice-sheets the wet delay is expected to be negligible and we will evaluate the dry-delay variability from local weather station records.

Finally, the spacecraft attitude knowledge, baseline dilation and differential antenna phase changes can all be modeled as a single effective quadratic "tilt" characteristic across the swath. We have adopted and adapted a calibration approach developed for WSOA whereby measurements from a nadir-viewing

alitimeter is used to correct for this characteristic (in the case of WSOA the tilt was effectively linear for near-nadir angles) by finding "cross-overs" where the altimeter path falls within the interferometer swath within the decorrelation time of the scene. We have developed a dynamic simulation that simulates this calibration strategy over both Greenland and Antarctica using the proposed orbit and nominal input dynamics. Figure 2 shows an initial cross-track accuracy prediction. In the upper plot, the measured height and then corrected height across-track are depicted, with the altimeter "truth" noted as green points across the track. Note that the scale of the correction being applied is ~100m (in this instance a space-craft roll of 56 arcsec and a phase error of 10 deg is applied). The lower plot shows the residual post-calibration correction which falls well below our allocations in Table 3. While additional errors from atmospherics and snow-fall accumulation between altimeter/interferometer passes need to be integrated into the error budget this result is very encouraging.

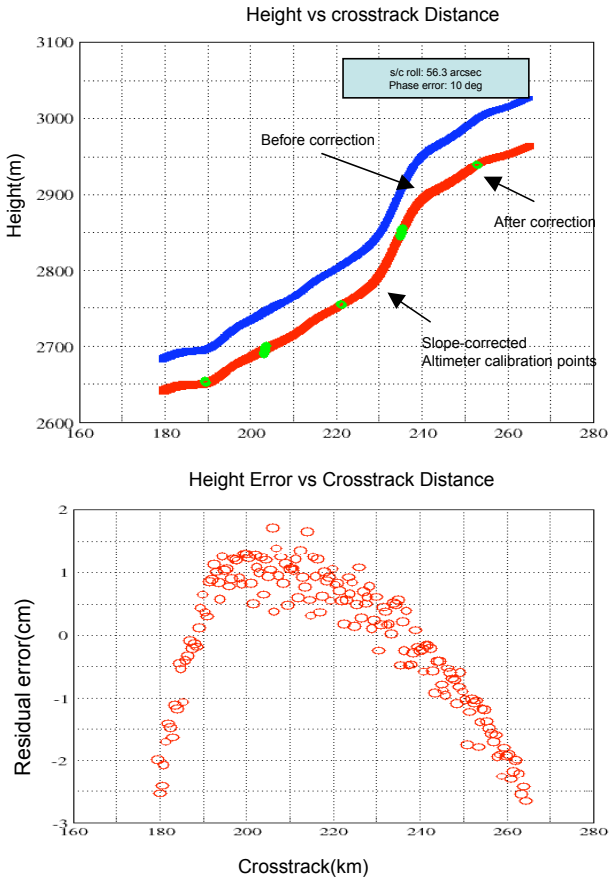

Figure 2: Cross-track calibration results for 1kmx1km pixel assuming interferometer radiometric errors & altimeter crossings +/- 10days.

IV. Demonstration and Technology Development

In addition to the mission feasibility studies, this program is developing and demonstrating the key technologies of the GLISTIN concept including the end-to-end measurement technique and associated processing. A block diagram of the key development, the digital antenna array, is shown in Figure 3. The antenna will be integrated into a simple radar system, mounted on a positioner at the JPL mesa facility, and used to collect an interferometric image. The demonstration antenna will be a 1m long (0.25 of the spaceborne length) full-height array (1.1m, 16 receive "sticks" and 1 transmit "stick"). Dedicated digital receivers will be integrated with each antenna stick and a 0.5m interferometric baseline will be synthesized by interfering the beamformed returns from the upper and lower halves of the array. An interferometric image will be produced through a combination of digital beam-forming for the fine-scale coupled with elevation scanning on a coarse scale using the positioner. Azimuth scanning will be achieved by rotating the positioner in that axis.

The two key sub-elements of the demonstration are the antenna aperture and the integrated digital receiver. Figure 4 shows a model of the integrated DBF antenna as a back view. These efforts are summarized subsequently and, as the development matures, will be the subject of future reporting. All other hardware is for the demonstration but not considered a technology challenge within the context of the IIP.

A. Antenna Requirements and Technology

The development of a 1m x 4m aperture at Ka-band is a challenging task. The first step is to decide which antenna technology will be used. This decision is largely influenced by mass, loss, profile – all of which must be very low – and compatibility with the system's digital beamforming network. A waveguide slot array was selected as the best candidate to meet these requirements.

It is envisioned that the GLISTIN 1m x 4m spaceborne aperture will be subdivided into four 1m x 1m waveguide slot array panels for deployment, with each panel consisting of 160 slots by 160 slots. Existing technologies, however, do not permit fabrication of a complete 1m x 1m array panel in a single step. So, each panel must be comprised of several smaller subarrays that are mounted on an external support frame. The full 1m x 4m aperture would then be connected through separate power divider networks attached to the back of the array.

Given the complexities involved in fabricating the full 1m x 4m aperture, the development path must be selected carefully in order to identify potential problems early in the project. In order to test the digital beamforming radar on Earth, a 1.1m x 1m array panel (taller to include a separate transmit "stick") was chosen for the demonstration aperture. Given limitations in the current manufacturing technology a two-step approach to the implementation was taken:

1. A small (10x40 slot) prototype would be produced and tested, thereby verifying the manufacturability and the design.
2. After a successful prototype, the full array would be designed and built. Nominally the array will be subdivided into "tiles" as shown in Figure 5. The 6 40x80 tiles and 2 50x80 tiles are connected on the back with a power combiner network to electrically create 17 (1 transmit and 16 receive) 10x160 "sticks".

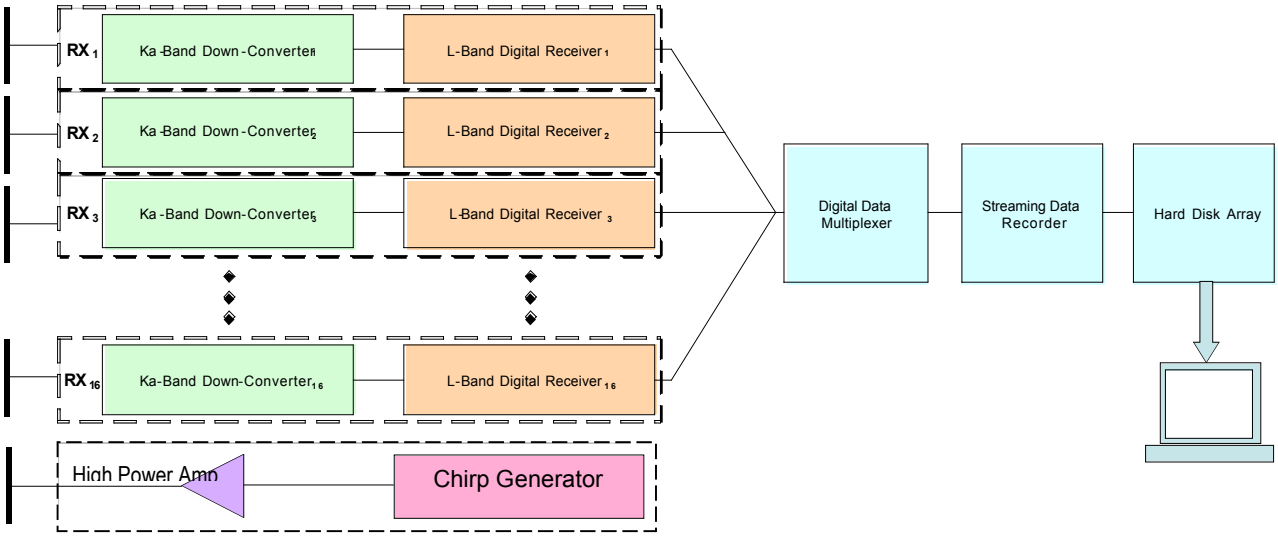

Figure 3: Technology demonstration block diagram.

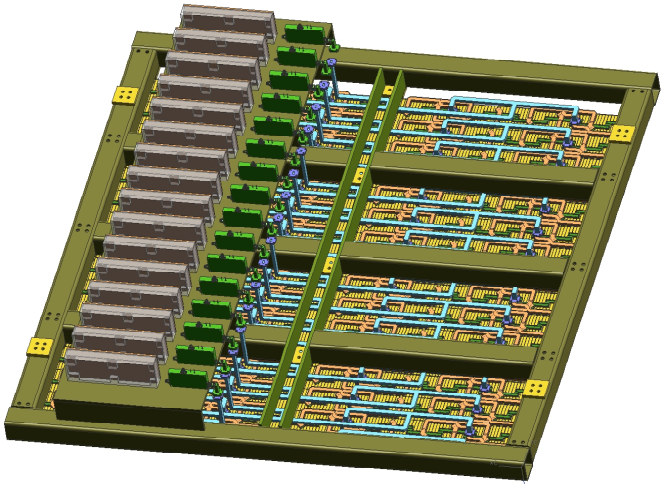

Figure 4: Model of antenna array mounted on frame with integrated receivers on back.

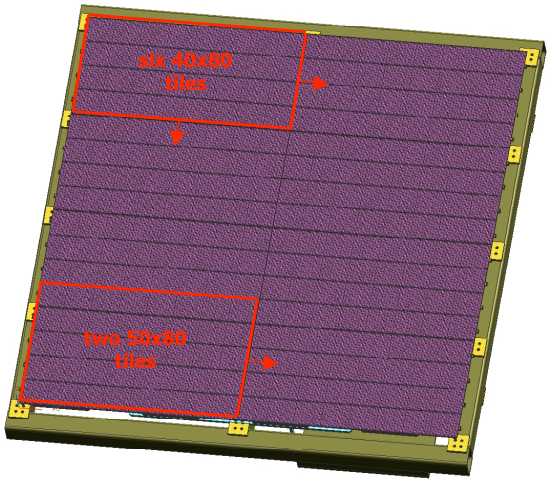

Figure 5: Subdivision of array into 6 40x80 and 2 50x80 "tiles".

B. Prototype Design and Implementation

In the design process, an infinite array analysis was employed [4]. In such a model, the external mutual coupling between radiating elements is modeled by considering each slot to be embedded in an infinite array. The accuracy of the infinite array model becomes better as the array size becomes bigger and its validity has been established even for a small 7x7 array [4]. Based on Scharstein's work [5], we believe that the use of the infinite array model for external mutual coupling employed in the GLISTIN antenna may introduce errors in slot voltages only in the outermost two rows and two columns with minimal error in the input reflection coefficient. A number of computer programs were developed to solve the pertinent coupled integral equations for the slot aperture electric field by the method of moments. For the infinite array mutual coupling problem, our computer program was validated by comparing our results with those of Ansoft High Frequency Structure Simulator (HFSS).

Design and Fabrication

The smallest subarray unit is 10x10 elements, and four of these are combined to make the next subarray level up: a 10x40 array. This subarray was selected as the prototype to validate both the model and fabrication techniques. The design and modeling applied an infinite array modeling analysis to moment method and HFSS simulations of a 10x10 array showing good agreement. Radiation patterns were also computed using the pattern multiplication principle before finalizing the design and solid models. The results of this prototype cycle will be used to scale up to the larger 40x80 and 50x80 subarray tiles which will then be used to populate the 1.1m x 1m aperture of the demonstration antenna.

There are two main components in the prototype design: the radiating and coupling slots, and a four-way equal-split corporate feed network that feeds each 10x10 subarray in the larger 10x40 prototype array. The feed network was designed using standard WR-28 waveguide dimensions to facilitate calibration and measurement. The main components of the feed network are H-plane Tee septum power dividers, H-plane bends, equal-length waveguide runs to each subarray, and an E-plane Tee at the input to the 10x40 subarray. All components in the feed network are tuned to the required operating frequency of 35.66GHz.

An additional feature introduced into the feed network was an E-plane phase "trombone", whose main function is to equalize the phase to each 10x10 subarray with shims, and is required only if fabrication tolerances create phase imbalances. However, by adding mounting flanges at the trombones, it is not only possible to measure the equality of amplitude and phase to each subarray – but also to measure the individual performance of each 10x10 subarray. A standard WR-28 waveguide calibration kit can easily be used to achieve this. An aluminum cover with two E-plane bends is used to close off the trombone for full 10x40 subarray operation.

In conjunction with the electrical design, it is necessary to make the part compatible with the aluminum dip brazing fabrication process. In order for this process to go smoothly and reliably, several features must be included in the mechanical design of the components. Working closely with the vendor, these details were finalized and a 3-D solid model was created. Shown in Fig. 6, this solid model was also used to program the CNC machines.

The dip-brazing process involves first machining the various layers of the array in aluminum and then fusing them together by dipping them in a 1000°F salt bath for several seconds. The part is then thoroughly cleaned to remove excess salt from the interior followed by some final machining of the mounting fixtures. The final prototype, shown in its feed network test configuration, is given in Figure 7.

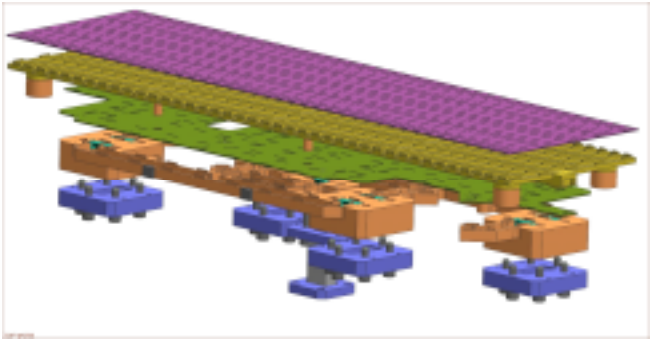

Figure 6: Three-dimensional model of 10x40 subarray.

Figure 7: Final brazed 10x40 subarray shown in feed network test configuration.

Measurements

Overall, the results were very good. The input match for the full 10x40 subarray, given in Figure 8, shows the resonant frequency is about 1% below the design frequency of 35.66GHz, and within simulation and fabrication tolerance errors.

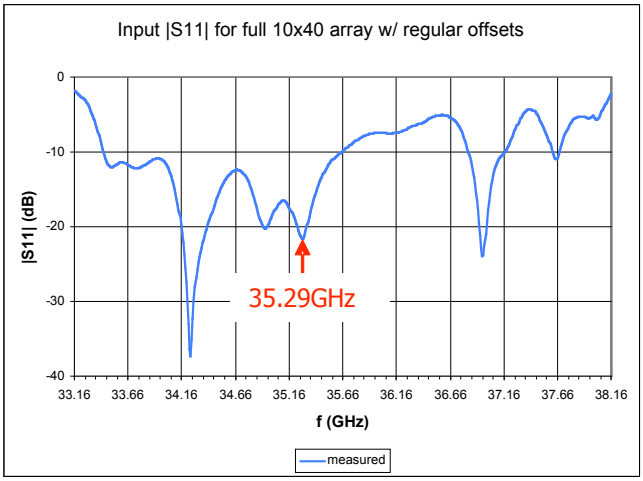

Figure 8: Input match for 10x40 subarray.

The E- and H-plane measured patterns at 35.66GHz are shown in Figures 9 and 10, respectively, and show good agreement with our *a priori* modeling. The measured E-plane beamwidth of 1.73° agrees very well with the predicted 1.70°. Similarly, the measured H-plane beamwidth of 6.98° agrees very well with the predicted 6.87° and meets the requirement for a beamwidth greater than 6.8°.

Subsequent moment method calculations suggest that it may be possible to adjust all the slot lengths by 1% to compensate for the missed resonant frequency. While this is the simplest and most appealing of all possible solutions, it also does not take into account fabrication repeatability. Due to schedule constraints and risk mitigation we decided to use the prototype design unaltered for the demonstration array and adjust the radar electronics accordingly to a new center frequency of 35.06GHz. This design choice represents a compromise between antenna pattern, return loss and avoidance of spurious mixing products in the radar design. However, in parallel with the demonstration array production, we intend to build a second 10x40 prototype with each 10x10 tuned to a different center frequency based on the data gathered from the prototype implementation. In this manner we will

establish repeatability of the design for an eventual spaceborne implementation.

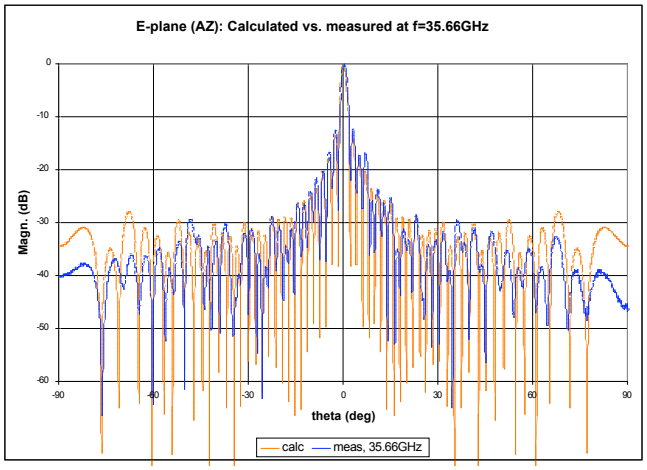

Figure 9: E-plane patterns for 10x40 subarray.

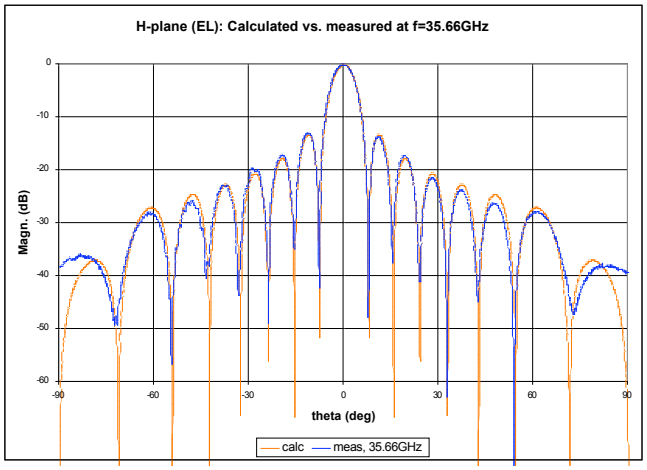

Figure 10: H-plane patterns for 10x40 subarray.

C. Radar Electronics

The GLISTIN radar electronics include a transmitter, 16 receive elements and a data acquisition system (DAQ). The transmitter is a two-stage up-converter composed of off-the-shelf, connectorized components. A custom JPL-designed digital chirp generator (DCG) provides the input waveform. A solid-state power amplifier provides the final gain stage yielding an output power of 8W. From a technology standpoint, the major development is the 16 receive elements utilized for digital beamforming. In the design of the receivers every effort is being made to be consistent and relevant to the potential spaceborne application including the selection of space-qualified (or those with a qualification path) for the critical components. A comparison of the demonstration versus the spaceborne requirements is shown in Table 4. Note that it is primarily the timing that differs due to the short range of operation when compared with a spaceborne application; it also keeps the data rate manageable. Note that, in the spaceborne scenario, data rate is a serious issue and we will conduct a study of on-board-processing and data downlink alternatives in Year 3 of this program. Finally, for the demonstration we have increased the bandwidth to 80MHz (from 40MHz) to have greater resolution for the demonstration.

Logically, the receivers are comprised of two components: a Ka-band down-converter and an L-band digital receiver. In the demonstration configuration the Ka-band down-converter accepts an 80 MHz input centered at 35.06 GHz and translates it to 1.26 GHz. Down-conversion is achieved through the use of an even-harmonic mixer, which utilizes a local oscillator (LO) frequency at 1/2 that of a fundamental mixer, thereby simplifying the distribution of the LO. The down-converters are custom designed, connectorized units provided by a vendor. The digital receiver filters and adjusts signal amplitude before digitizing the signal at 10bits resolution. Digitization is accomplished through bandpass sampling of the 1.26GHz signal at 240 MHz. These data are passed through a 1 to 4 demultiplexer and then buffered through a FPGA before transitioning to the DAQ. Data from all 16 channels are aggregated over a front panel data port (FPDP) bus, translated to an optical standard and then passed to a consumer-off-the-shelf (COTS) data system for storage onto a hard disk array.

TABLE 4: KEY RECEIVER REQUIREMENTS

Parameters	Requirement	
	Flight	Demo
Bandwidth	40 MHz	80 MHz
Rx Window	178 usec	50 usec
PRF	4 kHz	500 Hz
Noise Figure	4.5 dB	4.5 dB
ENOB	> 7 bits	> 7 bits
ADC Jitter	< 0.01 nsec	< 0.01 nsec

Initial testing of the down-converters shows performance that meets or exceeds specifications (see Table 5).

The prototype L-band receiver board is in-house (Figure 12) and being tested before final production of the 16 receivers. Figure 13 shows initial test results, whereby a 1.26GHz CW signal was input and data collected on a logic analyzer at the FPDP interface. The plot shows a near ideal signal-to-noise performance for the 10bit dynamic range, and no spurious signals above the noise floor. We intend to send the production design out for fabrication in the Fall of 2007.

TABLE 5: KA-BAND DOWN-CONVERTER REQUIREMENTS AND MEASURED PERFORMANCE

	Requirement	Measurement
Center Frequency	35.06 GHz	35.06 GHz
Gain	30 dB	30 dB
P1dB	0 dBm	+3 dBm
Image Rejection	20 dB	40 dB
Power Consumption	400 mA @ +8 V	300 mA @ +8 V

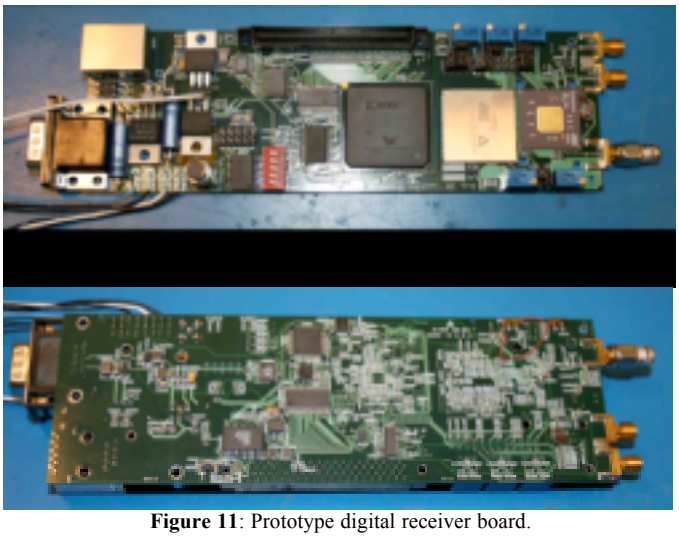

Figure 11: Prototype digital receiver board.

V. Summary

This paper updated both mission calibration analyses and technology development for the GLISTIN IIP. We have found very encouraging results in simulation that the calibration strategy we are pursuing will yield results that fall within the tight accuracy requirements.

The technology development is proceeding well, with a successful antenna prototype having been manufactured and demonstrating good performance during testing. The center frequency was slightly below design, an issue we anticipated as a likelihood, and part of the rationale behind having an intermediate prototype. Our response to the frequency tuning result is to proceed with the demonstration antenna manufacture at a frequency mutually agreeable between the prototype antenna design and the radar electronics. In parallel a second prototype will prove our ability to scale the slot-spacing and the center frequency in a deterministic manner.

Additionally, the development of the radar electronics, most notably the digital receivers, is well under way and initial testing shows good performance. Ultimately 16 of these receivers will be mounted on the back of the antenna array and used to digitally beamform in elevation as a cohesive and phase calibrated unit. This will prove not only the technology performance, but also the entire interferometric digital beamforming concept.

Acknowledgment

This research was carried out at the Jet Propulsion Laboratory, California Institute of Technology, under a contract with the National Aeronautics and Space Administration.

References

[1] D.Moller , B. Heavey, R. Hodges, S. Rengarajan, E. Rignot, F. Rogez, G. Sadowy, M. Simard, M. Zawadzki, "The Glacier and Land Ice Surface Topography Interferometer (GLISTIN): A Novel Ka-band Digitally Beamformed Interferometer", ESTC '06 Conference, University Park, Maryland 2006

[2] G.Sadowy, B.Heavey, D. Moller, E. Rignot, M. Zawadzki, S. Rengarajan, "Technology Demonstration of Ka-band Digitally-Beamformed Radar for Ice Topography Mapping", IEEE Aerospace Conference, Big Sky Montana, 2007

[3] B.D. Pollard, E. Rodríguez, L. Veilleux, T. Akins, P. Brown, A. Kitiyakara, M. Zawadski, S. Datthanasombat and A. Prata, Jr, 2002: The wide swath ocean altimeter: radar interferometry for global ocean mapping with centimetric accuracy, Proceedings of the 2002 Aerospace Engineering

[4] R. J. Mailloux, Phased Array Handbook, Second Edition, Artech House, Norwood, MA, 2005.

[5] R. W. Scharstein, "Mutual coupling in a slotted phased array, infinite in E-plane and finite in H-plane," IEEE Trans. Antennas Propagation, vol.38, pp. 1186-1191, Aug. 1990.